

# Direct Detection of Reactive Nitrogen Species in Experimental Autoimmune Uveitis

Sun Ryang Bae, MD<sup>1</sup>, Guey Shuang Wu, PhD<sup>2</sup>, Alex Sevanian, PhD<sup>3</sup>, Brian E. Schultz, PhD<sup>4</sup>,  
Ehud Zamir, MD<sup>2</sup>, Narsing A. Rao, MD<sup>2</sup>

*Department of Ophthalmology & Laboratory of Visual Science, Daejon St. Marys Hospital<sup>1</sup>, Daejon, Korea,  
Department of Ophthalmology<sup>2</sup> and Molecular Pharmacology and Toxicology<sup>3</sup>, Keck School of Medicine,  
the University of Southern California, Los Angeles, CA,  
Department of Chemistry and Chemical Engineering, California Institute of Technology<sup>4</sup>, Pasadena, CA*

**Purpose:** Demonstrate unequivocally the generation of nitric oxide in experimental autoimmune uveoretinitis by electron spin resonance spectroscopy (ESR) using ferrous iron complex of N-methyl-D-glucamine dithiocarbamate, (MGD)<sub>2</sub>-Fe<sup>2+</sup>, as a spin trap.

**Methods:** Experimental autoimmune uveitis was induced in Lewis rats, and at the peak of the intraocular inflammation, the animals received intravitreal injections of the spin trap. The retina and choroid dissected from the enucleated globes were subjected to ESR. Similarly, the retina and choroid obtained at the peak of experimental autoimmune uveo-retinitis (EAU) were placed in a vial containing luminol, and chemiluminescence was counted on a Packard liquid scintillation analyzer.

**Results:** The ESR three-line spectrum (g=2.04; a<sub>N</sub>=12.5 G) obtained was characteristic of the adduct [(MGD)<sub>2</sub>-Fe<sup>2+</sup>-NO]. The majority of this signal was eliminated by the inducible nitric oxide synthase (iNOS) specific inhibitor aminoguanidine injected inflamed retina was detected when compared with that of the non inflamed controls. The chemiluminescent activity was further increased two-fold by the addition of bicarbonate to the inflamed retina; the phenomenon is attributable only to the presence of a high steady-state concentration of peroxynitrite.

**Conclusions:** The study shows an unequivocal presence of nitric oxide in EAU retina and choroid and the generation of peroxynitrite. High levels of these reactive nitrogen species generated in the inflamed retina and choroids are certain to cause irreversible tissue damage, especially at the susceptible sites such as photoreceptors.

*Korean Journal of Ophthalmology 21(1):21-27, 2007*

**Key Words:** Electron spin resonance spectroscopy, Luminol chemiluminescence, Nitric oxide, Peroxynitrite, Spin trapping

Uveitis is a complex intraocular inflammatory process primarily involving the uvea, retina, and other intraocular structures. This intraocular inflammation can be either acute or chronic and is readily induced in laboratory animals by sensitization with the retinal soluble protein S-antigen. The resultant inflammation is known as experimental autoimmune uveo-retinitis (EAU).<sup>1</sup> Previously, in EAU, we quantified the

nitric oxide (NO) production by the Griess reagent, and we and others evaluated the inducible nitric oxide synthase (iNOS) expression as the means of NO production in inflammation.<sup>2-6</sup> Although quantification of nitrite, nitrate, nitrosylhemoglobin, and methemoglobin generally reflects NO production in the biological system, interference in these assays by the tissue components is well known. Nitric oxide synthase presumably takes L-arginine as a substrate, converting it to NO and L-citrullin. However, in recent years, this direct link between NOS and NO was somewhat weakened by several new findings: 1) Nitric oxide synthase does not directly synthesize NO; rather, it synthesizes nitroxyl anion (NO<sup>-</sup>), which can subsequently be converted to NO in the presence of superoxide dismutase (SOD);<sup>7</sup> and 2) The quantity of NOS present does not directly reflect the amount of NO produced.<sup>8</sup> Therefore, a direct means of establishing the generation of NO in EAU is necessary.

*Received:* October 20, 2006    *Accepted:* February 2, 2007

Reprint requests to Sun Ryang Bae, MD, Phd. Department of Ophthalmology & Laboratory of Visual Science, College of Medicine, The Catholic University of Korea, Daejon St. Marys Hospital, 520 Daehungdong, Jung-gu, Daejon 301-723, Korea. Tel: 82-42-220-9590, Fax: 85-42-252-3215, E-mail: sunrbae@yahoo.com

\* This study was supported in part by grant EY 12363, National Institute of Health, Research to Prevent Blindness, New York, New York, and MOCIE through the Bio-Medicinal Research Center at Pai Chai University, South Korea.

Nitric oxide is a paramagnetic species that binds with high affinity to a variety of metal chelates. Therefore, electron spin resonance (ESR) spectroscopy with spin trapping reveals a direct evidence of  $\cdot\text{NO}$  presence. ESR can also specifically detect  $\cdot\text{NO}$  and distinguish it from three other redox forms. Two dithiocarbamate derivatives have frequently been used in the trapping of  $\cdot\text{NO}$  in living tissues.<sup>9-11</sup> These are ferrous iron complexes of N-methyl-D-glucamine dithiocarbamate,  $(\text{MGD})_2\text{-Fe}^{2+}$ , and diethyldithiocarbamate,  $(\text{DETC})_2\text{-Fe}^{2+}$ . The high binding constant and water solubility of  $(\text{MGD})_2\text{-Fe}^{2+}$  and the stability of the corresponding adduct  $[(\text{MGD})_2\text{-Fe}^{2+}\text{-NO}]$  have made it possible to detect low concentrations of  $\text{NO}$  formed in biological systems.<sup>12-14</sup>

Chemiluminescence is a photon emission process that is specifically enhanced by the presence of 5-amino-2,3-dihydro-1,4-phthalazinedione (luminol).<sup>15,16</sup> It has been widely used in the past in the detection of reactive radical species such as  $\text{O}_2\cdot^-$ , hydrogen peroxide, and the hydroxyl radicals released from cells and tissues.<sup>15-19</sup>

In vitro, the  $\cdot\text{NO}$  and  $\text{O}_2\cdot^-$  radicals are known to combine to form  $\text{ONOO}\cdot$ ; the rate of the combination reaction is limited only by diffusion ( $K=3.7\times 10^7$  M/s).<sup>20</sup> Peroxynitrite formation in vivo, however, is more difficult to detect, since  $\text{ONOO}\cdot$  is protonated with decomposition at physiological pH. It has recently been shown that in alkaline conditions (pH>9), the half-life of  $\text{ONOO}\cdot$  is considerably prolonged.<sup>20</sup> Therefore, this type of stabilization could facilitate the detection of  $\text{ONOO}\cdot$  generated in vivo. It has been reported that  $\text{ONOO}\cdot$  can induce luminol chemiluminescence that is inhibited by SOD or urate. It has further been shown that the bicarbonate/luminol system can specifically discern the presence of  $\text{ONOO}\cdot$  in the pool of reactive species by the formation of a labile intermediate  $\text{ONOOC(O)O}$  between  $\text{ONOO}\cdot$  and bicarbonate. This bicarbonate luminol adduct then decomposes to the active radical species, increasing the quantum yield to at least 2-fold from that of  $\text{ONOO}\cdot$  without bicarbonate.<sup>21</sup> Since no other reactive species released by the inflammatory phagocytes display this phenomenon, the extent of this increase signifies the presence of  $\text{ONOO}\cdot$  in the active radical pool.

In this study, we used ESR spin trapping with the  $(\text{MGD})_2\text{-Fe}^{2+}$  complex to unequivocally detect the synthesis of  $\cdot\text{NO}$  in the EAU retina and choroid for the first time. In addition to establishing the g-values and hyperfine splittings of the EAU samples, several controls with or without a spin trap were evaluated. An authentic  $[(\text{MGD})_2\text{-Fe}^{2+}\text{-NO}]$  complex was also prepared chemically to aid in the characterization of this adduct in the EAU retina. We have also quantified the photon-emitting species generated at the inflammatory site by luminol chemiluminescence. Bicarbonate was introduced in these systems, and the increase caused by this addition was quantified to demonstrate for the first time that the luminescent reactive species were mostly  $\text{ONOO}\cdot$ .

## Materials and Methods

### Induction of EAU

The uveitogenic human S-antigen peptide, DTNLASS-TIIKEGIDRTVLG, was synthesized on 4-hydroxy-methylphenoxymethyl resin using an automated peptide synthesizer (model 430A; Applied Biosystems, Foster City, CA) and desalted on a Sephadex G-10 column (Sigma, St. Louis, MO).<sup>1</sup> The purity was assessed by reversed phase high performance liquid chromatography (Bio-Rad, Richmond, CA). Male Lewis rats, each weighing 150-175 g (VAF, Charles River Laboratory, Wilmington, MA), were given a hind foot-pad with 100  $\mu\text{g}$  of human S-antigen peptide in Freund's complete adjuvant to induce EAU, as previously described. At the time of immunization, each animal also received an intravenous injection of 1  $\mu\text{g}$  pertussis toxin (List Biological Laboratory, Campbell, CA) in 0.3 ml sterile saline. A total of 117 rats were immunized; another 12 were used as non-immunized controls. Immunized animals were sacrificed at the peak of inflammation, at between 12 and 13 days post-immunized. The eyes were enucleated, the anterior segments were removed, and the retina and choroid were collected. All procedures conformed to the Association for Research in Vision and Ophthalmology Resolution on the Use of Animals in Research.

### Electron spin resonance spectroscopy and spin trapping

All procedures involving a spin trap were conducted under dim light. The spin trap complex  $(\text{MGD})_2\text{-Fe}^{2+}$  was prepared in 0.01 M phosphate-buffered saline (PBS) with final concentrations of 13.5 mM  $\text{FeSO}_4\cdot 7\text{H}_2\text{O}$  and 86.0 mM MGD (Oxis, Portland, OR). Two 10  $\mu\text{l}$  doses each of  $(\text{MGD})_2\text{-Fe}^{2+}$  solution were injected into the vitreous cavity at different scleral sites. Similarly, two 10  $\mu\text{l}$  injections containing 0.01 M PBS only were made in the control animals. Ninety minutes after injection, the animals were sacrificed, the globes were enucleated, and the retina and choroids were removed. The retina and choroid from two eyes were combined and homogenized briefly (two seconds) in 0.4 ml of  $(\text{MGD})_2\text{-Fe}^{2+}$  solution before the mixture was transferred into the ESR tube (Wilmad, Buena, NJ). The tube was incubated at room temperature for 30 minutes, and the ESR measurement commenced immediately at the end of incubation. For the inhibition experiments with AG, the globes were injected intravitreally with two 10  $\mu\text{l}$  doses of 12 mM AG at different sites, two hours prior to injection of the spin trap  $(\text{MGD})_2\text{-Fe}^{2+}$ , as described above. An authentic  $(\text{MGD})_2\text{-Fe}^{2+}\text{-NO}$  complex was prepared chemically. Aliquots of the MGD and  $\text{FeSO}_4\cdot 7\text{H}_2\text{O}$  stock solution were mixed to yield final concentrations of 6 mM MGD and incubated with 10  $\mu\text{m}$  of the  $\cdot\text{NO}$  donor, S-nitroso-N-acetyl-penicillamine (SNAP; Cayman Chemical Company, Ann Arbor, MI); the reaction product was transferred into the ESR tube.

Electron spin resonance spectra were recorded at 77 K using a Varian E-109 Spectrometer (Varian Instruments, Palo Alto, CA) equipped with a TE-102 cavity and a cold-finger dewar. Other instrument settings were as follows: 20 mW microwave power, 9.28 GHz frequency,  $4 \times 10^4$  gain, 100 KHz modulation frequency, 4 G modulation amplitude, 128 ms time constant, and 2 minute scan time. Scanning was repeated at least four times. All ESR measurements were carried out using a combination of two eyes as one sample, and each measurement was repeated at least three or four times, using a total of six to eight eyes for each category of measurement.

### Measurement of luminol chemiluminescence

A stock solution of luminol (Sigma, St. Louis, MO) was prepared by first dissolving 1 mg of luminol in 100  $\mu$ l of dimethyl sulfoxide and then diluting it to 10 ml with 0.01 M PBS (pH 7.4). Exactly 400  $\mu$ l of the stock solution was diluted to 200 ml with 0.01 M PBS to provide the working solution. The final concentration of luminol in the working solution was 0.2  $\mu$ g/ml. The final concentration of dimethyl sulfoxide was 0.28 mM. All procedures were conducted under dark illumination.

Each sample, consisting of retinas and choroids collected from six eyes, was placed in a polypropylene counting vial, and 10 ml of luminol working solution was added immediately before counting. Chemiluminescence was counted on a Packard liquid scintillation analyzer (Packard Instruments, Downers Grove, IL) with the operating mode set on single photon counting. This mode sets the two photomultiplier tubes in out-of-coincidence counting, thereby maximizing the counting efficiency for weak photon emission. All scintillation vials and solutions used were dark-adapted overnight prior to use to reduce background counting. Samples were counted for one minute immediately after mixing with luminol. The counting was then repeated for several cycles until the counts were stabilized. For the bicarbonate and inhibitor experiments, the retina/choroid samples were first counted until maximal stable counts were established, and then sodium bicarbonate (50 mM final concentration), SOD (5,270 units; Sigma), N-nitro-L-arginine methyl ester (L-NAME, 1 mM final concentration, Sigma), and AG (5 mM final concentration, Sigma) were added. In these experiments, counts without the inhibitor were first established by counting for 15 to 20 minutes; the inhibitor was then introduced, and the counting resumed for an additional 50 to 60 minutes. Alternatively, a parallel counting procedure was employed. Briefly, two vials with the same amount of tissue were counted for 10 to 15 minutes, bicarbonate/inhibitor was added to one of the vial, and counting for both vials was resumed for 50 to 60 minutes thereafter. These two counting procedures yield similar results. Each experiment was repeated at least three times, using a total of 18 globes for each category of experiment.

## Results

Following an intravitreal injection of the freshly prepared spin trap  $(\text{MGD})_2\text{-Fe}^{2+}$  into the eyes of the EAU rats, a prominent three-line ESR spectrum ( $a_N=12.5$  G;  $g_{\text{iso}}=2.04$ ) was obtained (Fig. 1). The spectrum unambiguously indicated the adduct  $[(\text{MGD})_2\text{-Fe}^{2+}\text{-NO}]$  and was consistent with that reported in the postischemic heart.<sup>22,23</sup> There was no appreciable signal in either the normal controls or the EAU rats injected with 0.01 M PBS without the spin trap (Fig. 1). Control animals injected with the same concentration of  $(\text{MGD})_2\text{-Fe}^{2+}$  yielded a group of low intensity multicomponent signals that are not characteristic of any known radical species (Fig. 1). In this spectrum, one of the more obvious broad signals from control animals with the spin trap is unrelated to the  $[(\text{MGD})_2\text{-Fe}^{2+}\text{-NO}]$  triplet, and its identity is not known. This particular signal appears to be associated with the spin trap and some component of the naïve retina, irrespective of the development of uveitis, since the chemically synthesized retina-free  $[(\text{MGD})_2\text{-Fe}^{2+}\text{-NO}]$  adduct resulted in no such signal. In the inhibition experiment, AG, which is an iNOS specific inhibitor, considerably suppressed the triplet signal (Fig. 2); the intensity of the  $[(\text{MGD})_2\text{-Fe}^{2+}\text{-NO}]$  signal was reduced to one-tenth or less of the corresponding signal without the inhibitor. In this experiment, AG was injected two hours before the injection of the spin trap. Aminoguanidine injected either three or four hours before administration of the spin trap resulted in further suppression (data not shown). The authentic  $[(\text{MGD})_2$

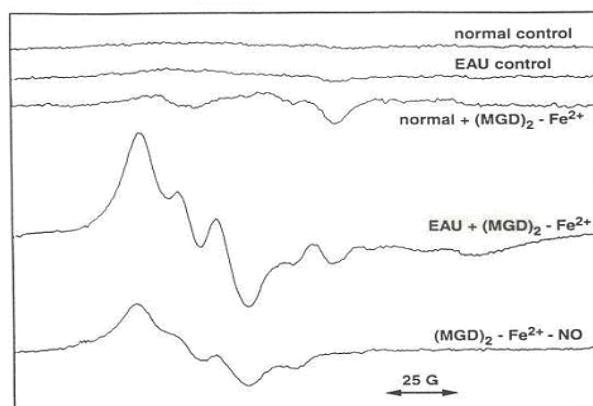


Fig. 1. ESR spin trapping of nitric oxide in the retina of EAU rats. ESR spectra were recorded from two inflamed retinas from Lewis rats 12 days post-immunization. Ninety minutes before sacrifice, the eyes were injected intravitreally with the spin trap,  $(\text{MGD})_2\text{-Fe}^{2+}$ ; after isolation, the retinas were incubated with  $(\text{MGD})_2\text{-Fe}^{2+}$  for 30 minutes before ESR recording. Each experiment was repeated three times, using a total of six eyes from different animals, and a representative spectrum is shown. normal control: non-immunized retina without spin trap; EAU control: EAU retina without spin trap; normal +  $(\text{MGD})_2\text{-Fe}^{2+}$ : non-immunized retina with spin trap; EAU +  $(\text{MGD})_2\text{-Fe}^{2+}$ : EAU retina with spin trap;  $(\text{MGD})_2\text{-Fe}^{2+}\text{-NO}$ : nitric oxide generated from SNAP in vitro reacted with spin trap.

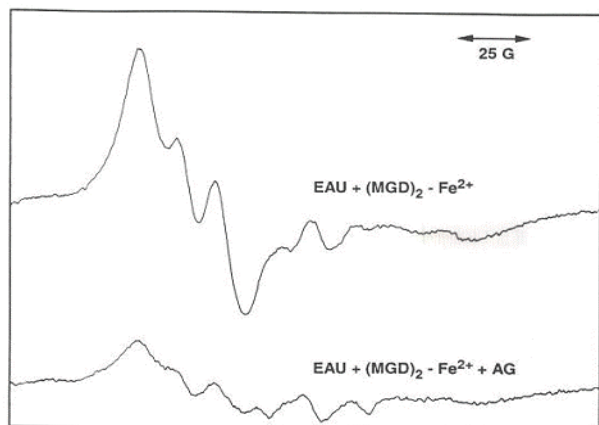


Fig. 2. Effect of AG on the ESR spin trapping of nitric oxide in the EAU retina. Lewis rats with EAU were injected intravitreally with either AG or PBS (as control) two hours prior to the injection of the spin trap, (MGD)<sub>2</sub>-Fe<sup>2+</sup>. Following enucleation, the retina was incubated with the spin trap for 30 minutes before ESR measurement. Each experiment was repeated three times using a total of six eyes. Representative ESR spectra are shown. EAU+(MGD)<sub>2</sub>-Fe<sup>2+</sup>: EAU retina with spin trap; EAU+(MGD)<sub>2</sub>-Fe<sup>2+</sup>+ AG: EAU retina with spin trap plus AG.

-Fe<sup>2+</sup>-NO] prepared from the 'NO donor, SNAP, and the spin trap was also used in generation of an 'NO signal. With the concentration (10 μ M) of SNAP used, the triplet signal generated was not as intense as those seen in EAU tissues; nevertheless, the central g-value and hyperfine splitting are indicative of the [(MGD)<sub>2</sub>-Fe<sup>2+</sup>-NO] adduct and similar to those obtained from EAU eyes plus spin trap.

Luminol chemiluminescence was measured with the liquid scintillation analyzer set at out-of coincidence photon counting to maximize the counting efficiency. The chemiluminescence counting from a pool of six sets of retina and choroid at the peak of inflammation were on the order of 70,000 counts. The counts usually started immediately following the addition of luminol, reached a plateau in 20 minutes, and then decayed slowly after 40 minutes. A high level of counting persisted even after 60 minutes. At the plateau, the phagocytic chemiluminescence was at least six-fold higher than those derived from the non-inflammatory source (Fig. 3). The maximum counts obtainable for a specific inflammatory model appear to be highly dependent on the degree of inflammation. In the luminol chemiluminescence, after stabilization of the count, the exogenous addition of bicarbonate increased the maximal counts by more than two-fold and sustained this level for two hours thereafter. Without bicarbonate, the counts decayed after one hour. The enhancement in quantum yield by the introduction of bicarbonate has been attributed to the presence of ONOO<sup>-</sup> in the system and the subsequent formation of the labile intermediate ONOOC(O)O<sup>-</sup> to facilitate an increase in radical generation.<sup>21</sup> Using bicarbonate/luminol chemiluminescence in the inflamed

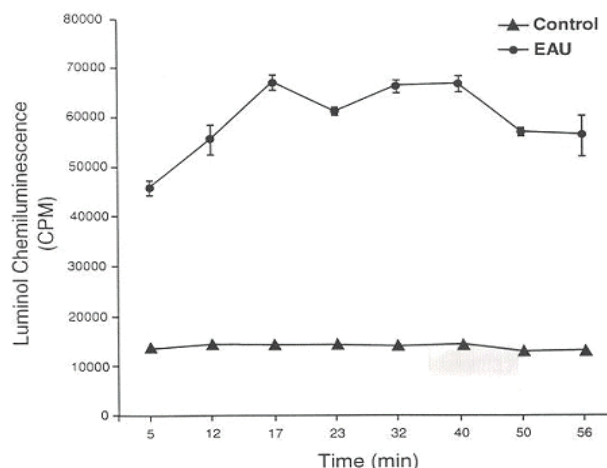
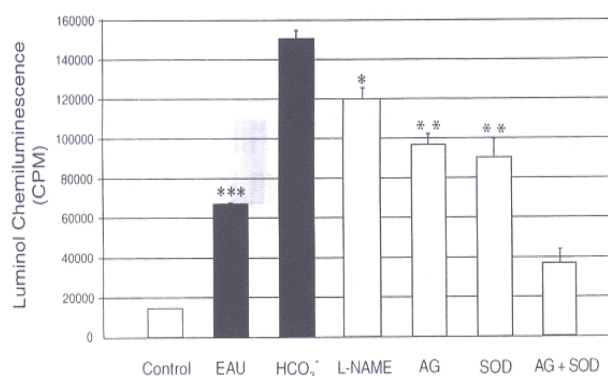


Fig. 3. Luminol chemiluminescence of EAU and control retinas. The retina and choroid from Lewis rats were collected at the peak of inflammation, 12 days post-immunization. Luminol (0.2 μ g/ml) was added to the tissues, and the chemiluminescence measurement commenced immediately with a Packard liquid scintillation analyzer set at an out-of coincidence mode for single photon counting. Six sets of retina/choroid were used for each sample, and each measurement was repeated three times, using a total of 18 eyes for each experimental category. Chemiluminescence is expressed as mean ± standard error for each category (n=3). An ANOVA single-parameter comparison between maximal chemiluminescent count in EAU vs. that in non-immunized control eyes indicated significance at p<0.0001.

retina, we evaluated the combined effects of the inhibitors SOD (5,270 units), L-NAME (1 mM), AG (5 mM), and AG (5 mM) + SOD (5,270 units). In these experiments, the counts without the inhibitors were first established, the desired amount of inhibitor was then introduced, and counting was resumed for 60 minutes thereafter. The extent of inhibition displayed with a particular inhibitor was subsequently confirmed with a second procedure. Two vials, one with and one without inhibitor, were counted in parallel. In some instances, the addition of the inhibitor caused a temporary surge in the counts; however, these counts rapidly returned to their respective levels, where they remained for at least 40 to 50 minutes. The two procedures yielded similar degrees of suppression. Using these procedures, 1 mM of L-NAME, an inhibitor of both constitutive and inducible NOS, was found to give 22% suppression. With either 0.1 or 2 mM concentrations of L-NAME, the change in the suppression level was found to be insignificant (data not shown). The inhibition was increased to 37% with 5 mM of AG, while SOD inhibited 40% of the chemiluminescent activity. In contrast with SOD, chemiluminescence was inhibited by 40%. A marked additive effect of 77% inhibition was seen with the combination of AG and SOD (Fig. 4).

### Discussion

In the present study, we obtained direct evidence of 'NO



**Fig. 4.** Effects of bicarbonate, SOD, L-NAME, AG, and AG + SOD on luminol chemiluminescence of EAU retina/choroids. The enhancement by the bicarbonate (50 mM, n=3) addition was first determined by counting six sets of retina/choroid with and without bicarbonate. The countings from the bicarbonate/luminol/retina system were then used as a background level for evaluating the inhibition displayed by SOD (5270 units/sample; n=3), L-NAME (1 mM, n=3), AG (5 mM, n=3), and SOD (5270 units) + AG (5 mM) (n=3). The counts without the inhibitor were established first, and then the inhibitor was added. The counting was continued until it became stabilized (60 minutes). A set of six retinas and choroids were used for one measurement. Measurements were repeated three times. All eyes used were 12 days post-immunization. Single-variable ANOVA was used to compare counts with the inhibitor groups to bicarbonate/luminol/chemiluminescence without inhibitors. \* $p < 0.005$ ; \*\* $p < 0.005$ ; \*\*\* $p < 0.0001$ . Control: non-immunized retina; EAU: EAU retina; HCO<sub>3</sub><sup>-</sup>: EAU retina + bicarbonate; L-NAME: EAU retina + bicarbonate + L-NAME; AG: EAU retina + bicarbonate + AG; SOD: EAU retina + bicarbonate + SOD; AG + SOD: EAU retina + bicarbonate + SOD + AG.

generation in the retina and choroid of EAU animals. The production of  $\cdot\text{NO}$  was unequivocally determined by ESR, using  $(\text{MGD})_2\text{-Fe}^{2+}$  complex as a  $\cdot\text{NO}$  trap. The three-line spectrum (central g value of 2.04 and hyperfine splitting of 12.5 G) obtained was characteristic of the adduct  $[(\text{MGD})_2\text{-Fe}^{2+}\text{-NO}]$ . The majority of this signal was eliminated by the AG intravitreally injected into the eye, as AG is a specific blocker for iNOS. In the inflamed retina, we also detected an approximately six-fold increase in chemiluminescent activity in comparison to those from the non-inflamed controls. These luminescent counts were further increased more than two-fold by the addition of bicarbonate to the isolated retina and choroid ex vivo, a phenomenon accounted for by the presence of a high steady-state concentration of ONOO<sup>-</sup>. Further, this luminescent activity was significantly inhibited by the addition of either AG or SOD separately, and markedly inhibited by the addition of AG and SOD combined. Again, this suggests that both  $\cdot\text{NO}$  and  $\text{O}_2$  participate in the formation of the major chemiluminescent species in the inflamed retina, namely ONOO<sup>-</sup>. Neither  $\cdot\text{NO}$  nor  $\text{O}_2$  alone was capable of directly producing luminol chemiluminescence.

Nitric oxide binds to  $(\text{MGD})_2\text{-Fe}^{2+}$  and forms the paramagnetic

$d^7$  state mononitrosyl iron complex  $[(\text{MGD})_2\text{-Fe}^{2+}\text{-NO}]$ , yielding the characteristic triplet ESR spectrum.<sup>24</sup> Thus,  $(\text{MGD})_2\text{-Fe}^{2+}$  is selective in trapping  $\cdot\text{NO}$ , since the trapping of  $\cdot\text{NO}$ , one of the redox forms of nitrogen monoxide, will result in a diamagnetic low spin  $D^8$  state undetectable by ESR spectroscopy. In the trapping of  $\cdot\text{NO}$  at the peak of inflammation, we obtained a prominent triplet signal of the  $[(\text{MGD})_2\text{-Fe}^{2+}\text{-NO}]$  adduct 10 times higher in intensity than that obtained from non-immunized animals injected with the same spin trap. Although the symmetry of the triplet in the ex vivo system is often not as distinct as those from the in vitro system [see, for example, ref. 24], the g-values and hyperfine splittings obtained are comparable to those reported in tissues for the same radical.<sup>25,26</sup> We have also obtained a signal from an authentic adduct, prepared independently from  $(\text{MGD})_2\text{-Fe}^{2+}$  and the  $\cdot\text{NO}$  donor SNAP; the spectrum and the g-value were very much in agreement with those from the EAU retinas. Little or no  $\cdot\text{NO}$  production is derived from injected  $(\text{MGD})_2\text{-Fe}^{2+}$ , as shown in control rats injected with  $(\text{MGD})_2\text{-Fe}^{2+}$ . This signal was also absent in EAU rats without the spin trap, indicating efficient trapping by  $(\text{MGD})_2\text{-Fe}^{2+}$  and subsequent stabilization and accumulation of  $(\text{MGD})_2\text{-Fe}^{2+}\text{-NO}$  in the retina.

In this experiment, intravitreally injected AG caused nearly complete suppression of the  $[(\text{MGD})_2\text{-Fe}^{2+}\text{-NO}]$  signal in the retina. Aminoguanidine, a nucleophilic hydrazine compound, is a known selective inhibitor of iNOS. The inhibitory action is believed to act on the enzymatic activity of iNOS.<sup>27</sup> Therefore, the marked suppressive effect of AG injected 3.5 hours prior to the sacrifice of the animal implies: first, that a large proportion of  $\cdot\text{NO}$  synthesis is L-arginine/iNOS-mediated, and second, that there is a relatively fast turnover of  $\cdot\text{NO}$  in the retina, so that the depletion of endogenous iNOS for at least 3.5 hours causes a significant reduction in the retinal  $\cdot\text{NO}$  concentration, as indicated by ESR spin trapping. In the presence of  $\text{O}_2$  at the site of  $\cdot\text{NO}$  generation, the major route of  $\cdot\text{NO}$  disappearance is by a fast combination reaction to yield ONOO<sup>-</sup>. In the absence of  $\text{O}_2$ ,  $\cdot\text{NO}$  is oxidized and disproportionated to yield nitrite and nitrate, which accumulate as stable products in tissues. With the concentrations injected into the eye for the present study, the  $(\text{MGD})_2\text{-Fe}^{2+}$  complex appears to compete favorably with other fates of  $\cdot\text{NO}$  in the retina, since the adduct  $[(\text{MGD})_2\text{-Fe}^{2+}\text{-NO}]$  obtained was in relatively high concentrations.

The  $(\text{MGD})_2\text{-Fe}^{2+}$  complex was delivered to the retina both by intravitreal injections to the eyes of live animals and by subsequent incubation of the isolated retinas with the  $(\text{MGD})_2\text{-Fe}^{2+}$  complex. Spin trapping of endogenously generated radicals within the retina has never been attempted in the past. The concentrations of  $(\text{MGD})_2\text{-Fe}^{2+}$  used in the present study were comparable to those reported for other tissues.<sup>9,11,14</sup> These  $(\text{MGD})_2\text{-Fe}^{2+}$  concentrations have been shown to pose no deleterious effects.<sup>9,11,28</sup> During the course of spin trapping, the free iron was unlikely to be present in the retina, since there is an excess amount of MGD present

for chelating exogenous iron (MGD:iron ratio=5:1). Therefore, it is safe to conclude that intravitreal injections of  $(\text{MGD})_2\text{-Fe}^{2+}$  complex will not lead to any deleterious reactions, including the stimulation of  $\text{NO}$  production. This assumption was subsequently verified by the experiment in which control animals injected with the same concentration of  $(\text{MGD})_2\text{-Fe}^{2+}$  gave no significant  $[(\text{MGD})_2\text{-Fe}^{2+}\text{-NO}]$  signal (Fig. 1).

Chemiluminescence counts for the phagocytic activity in inflammation appear to be highly system-dependent, possibly because of differences in the extent of inflammation and the size of tissues used. The reported maximal counts have been highly variable.<sup>19</sup> In this study, the chemiluminescence counts usually displayed a plateau at 20 to 40 minutes after the addition of luminol and decreased thereafter. The addition of bicarbonate to the inflamed retina rapidly increased the counts to more than two-fold. The half-life of  $\text{ONOO}^-$  was prolonged in the alkaline solution, since the protonation/decomposition reaction was largely eliminated. Therefore, the addition of bicarbonate stabilizes  $\text{ONOO}^-$ , thus facilitating the detection of  $\text{ONOO}^-$  in tissues. Moreover,  $\text{ONOO}^-$  appears to be the major species in the pool of reactive radical species, since the two-fold enhancement obtained by adding the bicarbonate is similar to the in vitro observations reported with the pure  $\text{ONOO}^-$  preparation.<sup>21</sup>

The exact pathway by which bicarbonate enhances the  $\text{ONOO}^-$  luminescence is not known. The light-emitting excited species is apparently produced by  $\text{ONOO}^-$  and  $\text{HCO}_3^-$  interactions. Although several thermodynamically feasible speculations have been advanced, the exact nature of this excited species is yet to be proved.<sup>29</sup> One fate for this unstable intermediate is to proceed to a facile decomposition that yields  $\text{O}_2^-$ .<sup>21</sup> Since the inhibitory effect of SOD (Fig. 4) indicates the participation of  $\text{O}_2^-$  in chemiexcitation, the increased production of  $\text{O}_2^-$  could, therefore, translate to a higher photon quantum yield.

The results of the bicarbonate luminol chemiluminescence indicate that although  $\text{ONOO}^-$  is short-lived at physiological pH ( $t_{1/2} < 1$  s), the inflammatory infiltrates are viable for a period of hours after the sacrifice of animals. During this period, these inflammatory cells were continuously activated to express NOS and NADPH oxidase and to produce  $\text{NO}$  and  $\text{O}_2^-$ . Superoxide is known to participate not by directly reacting to luminol, but rather by reacting with the luminol radical formed by the one-electron oxidation of luminol by oxidants, such as the  $\text{OH}^\cdot$  radical, lipid hydroperoxide, or other species with similar reactivity.<sup>17</sup> Therefore, the observed inhibitory effect of SOD can arise from the inhibition of  $\text{ONOO}^-$  formation from  $\text{O}_2^-$  and  $\text{NO}$ , or from the reaction of  $\text{O}_2^-$  with luminol radicals. In this context, the less than 50% inhibition exhibited by SOD might reflect the accessibility of SOD to the  $\text{O}_2^-$ -generating site in the retina within the short time frame between SOD addition and measurement of the photon emission.

The exogenous addition of L-NAME or AG inhibits the

function of NOS. Since AG is a specific inhibitor of iNOS and L-NAME is an inhibitor of both inducible and constitutive NOS, the larger suppression seen by AG might imply that iNOS is the predominant form in the production of  $\text{NO}$  in this system. However, even the suppression seen with AG is less than 50%. In this experiment, AG was added immediately before the addition of luminol and the measurement of chemiluminescence. Therefore, only the amount of  $\text{NO}$  newly synthesized within this time frame will be affected. The suppression, however, was more remarkable when instantaneous scavenging of  $\text{O}_2^-$  by SOD was added to this iNOS blocker.

Bicarbonate anion is an abundant constituent of the extracellular milieu, present at concentrations as high as 25 mM. Therefore, in biological systems, bicarbonate anion interacts rapidly with  $\text{ONOO}^-$  to form  $\text{ONOOC(O)O}^-$  and enhances the toxicity of  $\text{ONOO}^-$ , as seen in bicarbonate luminol chemiluminescence. Based on kinetic considerations, the  $\text{HCO}_3^-/\text{CO}$  pair should compete favorably with other biological targets, such as sulfhydryls, for reaction with  $\text{ONOO}^-$  in the extracellular space.<sup>29</sup> Heterolytic cleavage of  $\text{ONOOC(O)O}^-$  will also give rise to a potent nitrating agent that will regenerate  $\text{HCO}_3^-$ . This reaction is consistent with the catalytic effect of bicarbonate on  $\text{ONOO}^-$ -dependent nitration of aromatics, including tyrosine, reported previously.<sup>30,31</sup>

In summary, we have demonstrated the production of  $\text{NO}$  in EAU by ESR spin trapping. This method surpasses any other method for indirectly detecting the presence of  $\text{NO}$  species in the tissue. This reactive nitrogen species then forms the potent biological oxidant  $\text{ONOO}^-$  in the inflamed retina and choroid. Recognition of the species responsible for the tissue injury in EAU will aid in developing therapeutic interventions for the prevalent intraocular inflammations.

## References

1. Rao NA. Role of oxygen free radicals in retinal damage associated with experimental uveitis. *Trans Am Ophthalmol Soc* 1990;88:797-850.
2. Rao NA, Wu GS. Free radical mediated photoreceptor damage in uveitis. *Progress in Retina and Eye Res* 2000;19:41-68.
3. Zhang J, Wu GS, Rao NA. Role of nitric oxide (NO) in experimental autoimmune uveitis (EAU). *Invest Ophthalmol Vis Sci*. 1993;1000 abstr
4. Nathan C, Xie Q-W. Nitric oxide synthases: roles, tolls, and controls. *Cell* 1994;78:915-8.
5. Zhang J, Wu LY, Wu GS, et al. Differential expression of nitric oxide synthase in experimental uveoretinitis. *Invest Ophthalmol Vis Sci* 1999;40:1899-905.
6. Jacquemin E, de Kozak Y, Thillaye B, et al. Expression of inducible nitric oxide synthase in the eye from endotoxin-induced uveitis rats. *Invest Ophthalmol Vis Sci* 1996;37:1187-96.
7. Schmidt HHHW, Hofmann H, Schindler U, et al. No  $\text{NO}$  from NO synthase. *Proc Natl Acad Sci USA*. 1996;93:14492-7.

8. Komarov AM, Wink DA, Feelisch M, et al. Electron paramagnetic resonance spectroscopy using N-methyl-D-glucamine dithiocarbamate iron cannot discriminate between nitric oxide synthase. *Free Radic Biol Med* 2000;28:739-42.
9. Lai CS, Komarov AM. Spin trapping of nitric oxide produced in vivo in septic-shock mice. *FEBS Lett* 1994;345:120-4.
10. Zweier JL, Wang P, Samouilov A, et al. Enzyme-independent formation of nitric oxide in biological tissues. *Nature Med* 1995;1:804-9.
11. Komarov AM, Kramer JH, Mak IT, et al. EPR detection of endogenous nitric oxide in postischemic heart using lipid and aqueous-soluble dithiocarbamate-iron complexes. *Mol Cell Biochem* 1997;175:91-7.
12. Obolenskaya M, Yu, Vanin AF, et al. EPR evidence of nitric oxide production by the regenerating rat liver. *Biochem Biophys Res Commun* 1994;571-6.
13. Komarov AM, Lai CS. Detection of nitric oxide production in mice by spin-trapping electron paramagnetic resonance spectroscopy. *Biochim Biophys Acta* 1995;1272:29-36.
14. Bune AJ, Shergill JK, Cammack R, et al. L-arginine depletion by arginase reduces nitric oxide production in endotoxemic shock: an electron paramagnetic resonance study. *FEBS Lett* 1995;366:127-30.
15. Allen RC. Phagocytic leukocyte oxygenation activities and chemiluminescence: a kinetic approach to analysis. *Methods Enzymol* 1986;133:449-93.
16. Merenyi G, Lind J, Eriksen TE. The reactivity of superoxide ( $O_2^-$ ) and its ability to induce chemiluminescence with luminol. *Photochem Photobiol* 1985;41:203-8.
17. Radi R, Rubbo H, Thomson L, et al. Luminol chemiluminescence using xanthine and hypoxanthine as xanthine oxidase substrates. *J Free Rad Biol Med*. 1990;8:121-6.
18. Archer SL, Nelson DP, Weir EK. Simultaneous measurement of  $O_2^-$  radicals and pulmonary vascular reactivity in rat lung. *J Appl Physiol* 1989;67:1903-11.
19. Dowling EJ, Symons AM, Parke DV. Free radical production at the site of an acute inflammatory reaction as measured by chemiluminescence. *Agents Actions* 1986;19:203-7.
20. Beckman JS, Beckman TW, Chen J, et al. Apparent hydroxyl radical production by peroxynitrite: implications for endothelial injury from nitric oxide and superoxide. *Proc Natl Acad Sci USA* 1990;87:1620-4.
21. Radi R, Cosgrove TP, Beckman JS, et al. Peroxynitrite-induced luminol chemiluminescence. *Biochem J* 1993;290:51-7.
22. Wang P, Zweier JL. Measurement of nitric oxide and peroxynitrite generation in the postischemic heart. Evidence for peroxynitrite-mediated reperfusion injury. *J Biol Chem* 1996;271:29223-30.
23. Zweier JL, Wang P, Kuppusamy P. Direct measurement of nitric oxide generation in the ischemic heart using electron paramagnetic resonance spectroscopy. *J Biol Chem* 1995;270:304-7.
24. Xia Y, Zweier JL. Direct measurement of nitric oxide generation from nitric oxide synthase. *Proc Natl Acad Sci USA* 1997;94:12705-10.
25. Mulsch A, Vanin A, Mordvintcev P, et al. NO accounts completely for the oxygenated nitrogen species generated by enzymic L-arginine oxygenation. *Biochem J* 1992;288:597-603.
26. Kubrina LN, Mikoyan VD, Mordvintcev PI, et al. Iron potentiates bacterial lipopolysaccharide-induced nitric oxide formation in animal organs. *Biochim Biophys Acta* 1993;1176:240-4.
27. Corbett JA, McDaniel ML. Selective inhibition of inducible nitric oxide synthase by aminoguanidine. *Methods Enzymol* 1996;268:398-408.
28. Shinobu LA, Jones SG, Jones MM. Sodium N-methyl-D-glucamine dithiocarbamate and cadmium intoxication. *Acta Pharmacol Toxicol (Copenh)* 1984;54:189-94.
29. Denicola A, Freeman BA, Trujillo M, et al. Peroxynitrite reaction with carbon dioxide/bicarbonate: kinetics and influence on peroxynitrite-mediated oxidations. *Arch Biochem Biophys* 1996;333:49-58.
30. Gow A, Duran D, Thom SR, et al. Carbon dioxide enhancement of peroxynitrite-mediated tyrosine nitration. *Arch Biochem Biophys* 1996;333:42-8.
31. Zhang H, Joseph J, Felix C, et al. Bicarbonate enhances the hydroxylation, nitration, and peroxidation reactions catalyzed by copper, zinc superoxide dismutase. Intermediacy of carbonate anion radical. *J Biol Chem* 2000;275:14038-45.